ORGANIC LETTERS

2011
Vol. 13, No. 15
3840–3843

Planar Macrocyclic Fluoropentamers as Supramolecular Organogelators

Changliang Ren,[†] Shengyu Xu,[†] Jun Xu,[‡] Hongyu Chen,[‡] and Huaqiang Zeng*,[†]

Department of Chemistry and NUS MedChem Program of the Office of Life Sciences, 3 Science Drive 3, National University of Singapore, Singapore 117543, and Division of Chemistry & Biological Chemistry, School of Physical & Mathematical Sciences, Nanyang Technological University, 21 Nanyang Link, Singapore 637371

chmzh@nus.edu.sg

Received May 19, 2011

ABSTRACT

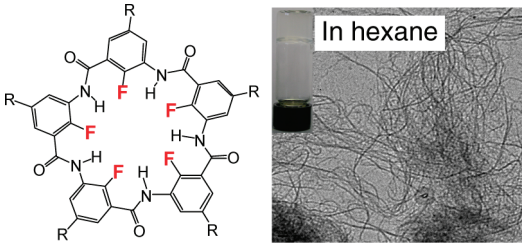

Despite their great diversities, 2D-shaped macrocycles that can serve as the organogelators have been surprisingly rare; two planar macrocyclic fluoropentamers designed by us were highly able to gelate organic solvents, largely derived from their strong tendency to form 1D stacked fibrillar structures stabilized by both interplanar H-bonds and $\pi-\pi$ stacking forces.

Low-molecular-weight organogelators (LMOGs) have promising applications in diverse areas ranging from structure-directing agents, drug delivery systems, sensors, catalysis, to electronic nanodevices.[1] Compared to the currently available large structural diversity of acyclic gelators,[1a−i] the emerging macrocyclic gelators have been much less studied.[1j] The hitherto discovered macrocyclic gelators or their simply modified derivatives mostly have been based on well-known three dimensionally (3D) shaped molecules including calixarene,[2a,b] cyclodextrin,[2c] cyclophane,[2d] resorcinarene,[2e] cucurbit[7]uril,[2f] crown ether,[2g] and diimide[2h]- or dehydrobenzoannulene[2i]-based macrocycles, while 2D planar macrocyclic organogelators remain very limited with only one recent example known to us that derives from arylene ethynylene macrocycles.[2j,k] This inability of 2D-shaped macrocycles to form gels is in sharp contrast with their ability to form vesicles of varying sizes[3a−d] and with the significant gellating ability of other planar polycyclic molecules.[3e−g] Given the availability of diverse 2D-shaped macrocycles,[3h] the rare occurrence of their use as organogelators can be attributed to the general difficulty[1e,2h,2j] in the rational design of organogelators

[†] National University of Singapore.
[‡] Nanyang Technological University.

(1) (a) Abdallah, D. J.; Weiss, R. G. *Adv. Mater.* **2000**, *12*, 1237. (b) Weiss, R. G.; Terech, P. *Molecular Gels: Materials with Self-Assembled Fibrillar Networks*; Springer: New York, 2006. (c) Hirst, A. R.; Escuder, B.; Miravet, J. F.; Smith, D. K. *Angew. Chem., Int. Ed.* **2008**, *47*, 8002. (d) Llusar, M.; Sanchez, C. *Chem. Mater.* **2008**, *20*, 782. (e) Dastidar, P. *Chem. Soc. Rev.* **2008**, *37*, 2699. (f) Piepenbrock, M.-O. M.; Lloyd, G. O.; Clarke, N.; Steed, J. W. *Chem. Rev.* **2009**, *110*, 1960. (g) Smith, D. K. *Chem. Soc. Rev.* **2009**, *38*, 684. (h) Suzaki, Y.; Taira, T.; Osakada, K. *J. Mater. Chem.* **2010**, *21*, 930. (i) Steed, J. W. *Chem. Commun.* **2011**, *47*, 1379. (j) Cao, R.; Zhou, J.; Wang, W.; Feng, W.; Li, X.; Zhang, P.; Deng, P.; Yuan, L.; Gong, B. *Org. Lett.* **2010**, *12*, 2958.

(2) (a) Aoki, M.; Murata, K.; Shinkai, S. *Chem. Lett.* **1991**, 1715. (b) Becker, T.; Yong Goh, C.; Jones, F.; McIldowie, M. J.; Mocerino, M.; Ogden, M. I. *Chem. Commun.* **2008**, 3900. (c) Kida, T.; Marui, Y.; Miyawaki, K.; Kato, E.; Akashi, M. *Chem. Commun.* **2009**, 3889. (d) Becerril, J.; Burguete, M. I.; Escuder, B.; Luis, S. V.; Miravet, J. F.; Querol, M. *Chem. Commun.* **2002**, 738. (e) Haines, S. R.; Harrison, R. G. *Chem. Commun.* **2002**, 2846. (f) Hwang, I.; Jeon, W. S.; Kim, H.-J.; Kim, D.; Kim, H.; Selvapalam, N.; Fujita, N.; Shinkai, S.; Kim, K. *Angew. Chem., Int. Ed.* **2007**, *46*, 210. (g) Jung, J. H.; Kobayashi, H.; Masuda, M.; Shimizu, T.; Shinkai, S. *J. Am. Chem. Soc.* **2001**, *123*, 8785. (h) Nakagaki, T.; Harano, A.; Fuchigami, Y.; Tanaka, E.; Kidoaki, S.; Okuda, T.; Iwanaga, T.; Goto, K.; Shinmyozu, T. *Angew. Chem., Int. Ed.* **2010**, *49*, 9676. (i) Hisaki, I.; Shigemitsu, H.; Sakamoto, Y.; Hasegawa, Y.; Okajima, Y.; Nakano, K.; Tohnai, N.; Miyata, M. *Angew. Chem., Int. Ed.* **2009**, *48*, 5465. (j) Balakrishnan, K.; Datar, A.; Zhang, W.; Yang, X.; Naddo, T.; Huang, J.; Zuo, J.; Yen, M.; Moore, J. S.; Zang, L. *J. Am. Chem. Soc.* **2006**, *128*, 6576. For porphyrin-based metal-containing 2D planar macrocyclic gelators, see: (k) Norstrum, C. F. v.; Picken, S. J.; Schouten, A.-J.; Nolte, R. J. M. *J. Am. Chem. Soc.* **1995**, *117*, 9957. (l) Iavicoli, P.; et al. *J. Am. Chem. Soc.* **2010** *132*, 9350.

10.1021/ol201361f
Published on Web 07/11/2011

and to the lack of suitable designer protocols allowing the strong intermolecular interactions among macrocycles to be directionally controllable and precisely balanced to favor the formation of not only one-dimensional (1D) fibrillar nanostructures but also 3D entangled networks for extensive solvent entrapment.[1e,2h−2j,3i] Accordingly, new gelling agents often have been discovered serendipitously or produced by modifying the serendipitously obtained gelators.[1e]

A few new dimensions recently were added into the design aspects of supramolecular gelling agents. Dastidar[1e,4a] and McNeil[4b,c] adopted a de novo crystal engineering approach to create new gelators by design. This approach emphasizes the importance of 1D intermolecular interactions in inducing and maintaining gel formation,[3i] and such interactions believably can be extracted from the known crystal structures and applied to identify new types of gelators. Another de novo design strategy explores the host−guest chemistry to design responsive supramolecular gels. The prominent examples along this line include the use of cyclodextrin by Harade,[4d] crown ether by Huang and Liu,[4e] cucurbit[8]uril by Scherman,[4f] and protein−peptide interactions by Regan.[4g]

We recently designed and crystallized *C*5-symmetric fluoropentamer **1**[5] with its circular pentameric backbone[3h,6] enforced by intramolecular C−F···H−N H-bonds (Figure 1a−b).[6e,f] The aromatic backbone of **1** was revealed to be quite planar which should enhance interplanar $\pi-\pi$ interactions. In addition, every pentamer forms two intermolecular C═O···H−N H-bonds (2.50 Å, Figure 1b) with its nearest pentamer, leading to a dimeric ensemble where the average interplanar distance is as short as 3.1 Å. These H-bonds form as a result of comparatively much weaker C−F···H−N H-bonds, causing the two amide bonds in every pentamer to twist out of the pentameric plane to form stronger C═O···H−N H-bonds with the adjacent nearest pentamer. The weakness of C−F···H−N H-bonds can be further illustrated by a dimer molecule **1d** (Figure 1c) whose amide bond is twisted out of the aromatic plane by 45° in order to form stronger C═O···H−N H-bonds (2.17 Å) even in the presence of two stabilizing C−F···H−N H-bonds (F···H distances = 2.50 and 2.54 Å).

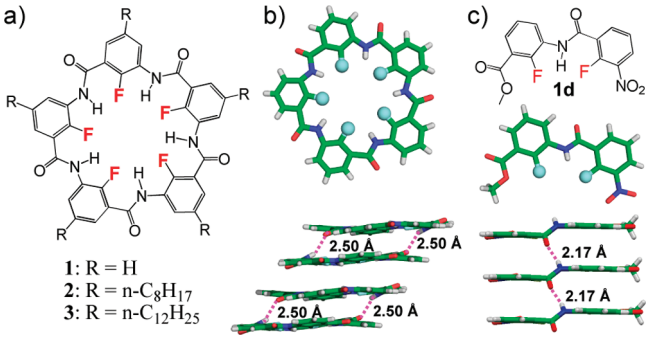

Figure 1. (a) Structures of fluoropentamers **1**−**3**. (b) Top and side views of crystal structure of **1**,[5] illustrating the formation of interplanar H-bonds of 2.50 Å in length. (c) Structure of dimer **1d**, and top and side views of its crystal structure, illustrating the formation of intermolecular H-bonds of 2.17 Å in length. Dotted cycles in (b) indicate the amide bonds that are twisted out of the plane to form stronger intermolecular H-bonds that enhance the interplanar aggregations.

Inferred from the existence of these interplanar H-bonds, shortened interplanar distance, and the planar aromatic backbone as found in pentamer **1** that exhibits very poor solubilities in all of the organic solvents, we envisioned that macrocyclic analogs derived from **1** that bear suitably modified hydrocarbon chains and enhanced solubilities could be gelators. Their gelating ability should derive first from their tendency to form 1D stacked fibrillar structures that are stabilized by both interplanar H-bonds and $\pi-\pi$ stacking forces (Figure 1c), followed by the intercolumnar association via hydrophobic hydrocarbon chains to form a 3D gelling network, resulting in the gel by trapping organic solvents through surface tension and capillary forces.

To test our hypothesis, pentamers **2** and **3** each can be synthesized after 15 steps starting from the commercially available 2-fluoro-3-nitrobenzoic acid (Scheme S1). The ability of **2** and **3** to serve as 2D planar macrocyclic gelators was examined in a variety of organic solvents by the "stable to inversion" method. In brief, the gelators and solvents were mixed in a sealed sample vial and heated in an oil bath

(3) (a) Shklyarevskiy, I. O.; Jonkheijm, P.; Christianen, P. C. M.; Schenning, A. P. H. J.; Meijer, E. W.; Henze, O.; Kilbinger, A. F. M.; Feast, W. J.; Guerzo, A. D.; Desvergne, J.-P.; Maan, J. C. *J. Am. Chem. Soc.* **2005**, *127*, 1112. (b) Seo, S. H.; Chang, J. Y.; Tew, G. N. *Angew. Chem., Int. Ed.* **2006**, *45*, 7526. (c) Hoeben, F. J. M.; Shklyarevskiy, I. O.; Pouderoijen, M. J.; Engelkamp, H.; Schenning, A. P. H. J.; Christianen, P. C. M.; Maan, J. C.; Meijer, E. W. *Angew. Chem., Int. Ed.* **2006**, *45*, 1232. (d) Ajayaghosh, A.; Varghese, R.; Praveen, V. K.; Mahesh, S. *Angew. Chem., Int. Ed.* **2006**, *45*, 3261. (e) Zang, L.; Che, Y.; Moore, J. S. *Acc. Chem. Res.* **2008**, *41*, 1596. (f) Wu, J.; Pisula, W.; Mullen, K. *Chem. Rev.* **2007**, *107*, 718. (g) Krieg, E.; Shirman, E.; Weissman, H.; Shimoni, E.; Wolf, S. G.; Pinkas, I.; Rybtchinski, B. *J. Am. Chem. Soc.* **2009**, *131*, 14365. (h) Qin, B.; Ren, C. L.; Ye, R. J.; Sun, C.; Chiad, K.; Chen, X. Y.; Li, Z.; Xue, F.; Su, H. B.; Chass, G. A.; Zeng, H. Q. *J. Am. Chem. Soc.* **2010**, *132*, 9564. (i) Pinacho Crisostomo, F. R.; Lledo, A.; Shenoy, S. R.; Iwasawa, T.; Rebek, J. *J. Am. Chem. Soc.* **2009**, *131*, 7402.

(4) (a) Das, U. K.; Trivedi, D. R.; Adarsh, N. N.; Dastidar, P. *J. Org. Chem.* **2009**, *74*, 7111. (b) Chen, J.; McNeil., A. J. *J. Am. Chem. Soc.* **2008**, *130*, 16496. (c) King, K. N.; McNeil, A. J. *Chem. Commun.* **2010**, *46*, 3511. (d) Deng, W.; Yamaguchi, H.; Takashima, Y.; Harada, A. *Angew. Chem., Int. Ed.* **2007**, *46*, 5144. (e) Ge, Z.; Hu, J.; Huang, F.; Liu, S. *Angew. Chem., Int. Ed.* **2009**, *48*, 1798. (f) Appel, E. A.; Biedermann, F.; Rauwald, U.; Jones, S. T.; Zayed, J. M.; Scherman, O. A. *J. Am. Chem. Soc.* **2010**, *132*, 14251. (g) Grove, T. Z.; Osuji, C. O.; Forster, J. D.; Dufresne, E. R.; Regan, L. *J. Am. Chem. Soc.* **2010**, *132*, 14024.

(5) Ren, C. L.; Zhou, F.; Qin, B.; Ye, R. J.; Shen, S.; Su, H. B.; Zeng, H. Q. *Angew. Chem., Int. Ed.* **2011**, in revision.

(6) (a) Yan, Y.; Qin, B.; Shu, Y. Y.; Chen, X. Y.; Yip, Y. K.; Zhang, D. W.; Su, H. B.; Zeng, H. Q. *Org. Lett.* **2009**, *11*, 1201. (b) Yan, Y.; Qin, B.; Ren, C. L.; Chen, X. Y.; Yip, Y. K.; Ye, R. J.; Zhang, D. W.; Su, H. B.; Zeng, H. Q. *J. Am. Chem. Soc.* **2010**, *132*, 5869. (c) Qin, B.; Chen, X. Y.; Fang, X.; Shu, Y. Y.; Yip, Y. K.; Yan, Y.; Pan, S. Y.; Ong, W. Q.; Ren, C. L.; Su, H. B.; Zeng, H. Q. *Org. Lett.* **2008**, *10*, 5127. (d) Qin, B.; Ren, C. L.; Ye, R. J.; Sun, C.; Chiad, K.; Chen, X. Y.; Li, Z.; Xue, F.; Su, H. B.; Chass, G. A.; Zeng, H. Q. *J. Am. Chem. Soc.* **2010**, *132*, 9564. (e) Qin, B.; Ong, W. Q.; Ye, R. J.; Du, Z. Y.; Chen, X. Y.; Yan, Y.; Zhang, K.; Su, H. B.; Zeng, H. Q. *Chem. Commun.* **2011**, *47*, 5419. (f) Qin, B.; Sun, C.; Liu, Y.; Shen, J.; Ye, R. J.; Zhu, J.; Duan, X.-F.; Zeng, H. Q. *Org. Lett.* **2011**, *13*, 2270.

until all of the gelators were dissolved. The solution was then cooled to 25 °C under ambient conditions. The samples were regarded as a gel if *no flow was observed* within 30 s after *inverting the vial*. By this method, solvents that can be gelated by **2** and **3** at room temperature are summarized in Table 1. In other solvents, **2** and **3** are either insoluble or too soluble (>25 mM), resulting in no gel formation. In both *n*-hexane and ethyl acetate, **3** carrying longer aliphatic side chains functions as a better gelator than **2** carrying shorter ones. Pentamer **2**, however, possesses a better gelating ability than **3** when diethyl ether, cyclohexane, and dioxane are used as the solvent, probably due to the much enhanced solubility of **3** in these solvents. The minimum gelation concentrations (MGCs) for **2** and **3** in *n*-hexane are as low as 2.67 and 1.61 mM, which correspond to 2.8×10^3 and 4.8×10^3 solvent molecules being efficiently trapped on average by just one macrocyclic gelator molecule of **2** and **3**, respectively.

Table 1. Minimum Gelation Concentrations for Pentamers **2** and **3** in Different Solvents at Room Temperature[a]

solvents	pentamer **2** (mM/wt %)	pentamer **3** (mM/wt %)
n-Hexane	2.67/0.51 (tr)	1.61/0.37 (tr)
Ethyl acetate	6.40/0.88 (op)	5.03/0.86 (op)
Diethyl ether	4.72/0.82 (op)	14.88/3.18 (op)
Cyclohexane	5.57/0.89 (tr)	S
Dioxane	5.70/0.69 (op)	20.40/3.02 (op)

[a] Abbreviations: S = soluble, tr = transparent, op = opaque.

Given that the absorption spectrum of the H-aggregate typically consists of a blue-shifted band with respect to the absorption by monomer, self-assembly of **2** and **3** in the organic solvents shown in Table 1 was investigated by UV−vis spectroscopy. Compared to the maximum adsorption (λ_{max}) value of 274 nm for both **2** and **3** in chloroform where no gelation occurs, a blue shift of 4−9 nm is observed in all the solvents in which they can form the gels (Table 1 and Figures S6 and S7). This blue shift is in accord with the H-type packing seen in the crystal structure (Figure 1b) and suggests both **2** and **3** assemble into the H-aggregates in forming the gels. Furthermore, except for **3** in dioxane, the λ_{max} values for **2** and **3** in *n*-hexane, ethyl acetate, cyclohexane, and dioxane are lower than those of **2** and **3** in chloroform (Figures S6 and S7), likely due to the better aggregation in these solvents with respect to chloroform whereby extensive aggregations of **2** also occur at ~1 mM and above (Figures S30 and S31).

Further examinations of variable temperature UV−vis data interestingly show that the absorbance of λ_{max} drops very quickly for **2** in *n*-hexane when temperature decreases from 25 to 0 °C (Figure 2a), suggesting stronger intermolecular aggregations occurring at lower temperature, while much smaller changes in λ_{max} value for **3** in *n*-hexane were observed (Figure 2b), indicating similar aggregation extents in **3** between 25 and 0 °C. Despite the fact that **3** actually is a better gelator than **2** in *n*-hexane at room

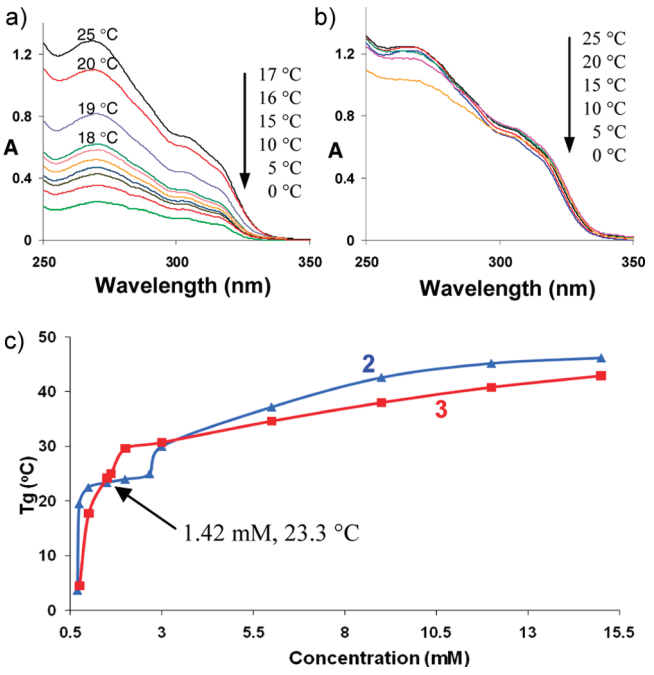

Figure 2. Temperature-dependent UV absorption spectra of (a) **2** and (b) **3** at 2×10^{-5} M in *n*-hexane. The determined gel−solution transition temperatures (T_g) for **2** and **3** in *n*-hexane at various concentrations. The data were the averaged value of two runs. The relative error for all of the T_g's is within 0.6 °C.

temperature (Table 1), the UV−vis data allow us to surmise that **2** possibly can gelate *n*-hexane better than **3** at 25 °C. To verify this postulate, gel−solution transition temperatures (T_g) for **2** and **3** in *n*-hexane were determined by the "falling drop" method.[7] Indeed, at the lower temperature end, **2** is a better gelator (Figure 2c). The intersection point of the two curves has a (1.42 mM, 23.3 °C) coordinate, suggesting that **2** and **3** are equal gelators and capable of gelating *n*-hexane at an MGC of 1.42 mM at 23.3 °C. At temperatures below 23.3 °C, **2** becomes more capable of gelating *n*-hexane. For instance, at 19.5 °C, the MGC of **2** was determined to be 0.75 mM, while the MGC of **3** extrapolated from the curve is 1.09 mM. Consistent with the very strong intermolecular aggregation that does not change significantly between 0 and 18 °C (Figure 2a), MGC values for **2** essentially remain constant around 0.70 mM over the same temperature range. In further accord with the dramatically increased λ_{max} values and apparently much weakened intermolecular aggregation from 18 to 25 °C, the MGC value of **2** increases radically from ~0.70 to 2.67 mM. This trend in intermolecular aggregation and MGC values in *n*-hexane was completely reversed in ethyl acetate. Specifically, the intermolecular aggregation inferred from UV−vis spectra is considerably enhanced for **3**, rather than **2**, between 0 and 25 °C (Figures S10 and S11).

(7) Debnath, S.; Shome, A.; Dutta, S.; Das, P. K. *Chem.—Eur. J.* **2008**, *14*, 6870.

Accordingly, **3** remains as a consistently better gelator of ethyl acetate than **2** at < 25 °C (Figure S5).

The solid state morphology of the gelling networks for the as-formed gels was visualized using the transmission electron spectroscopy (TEM) technique. Typically, the TEM grids were immersed in the gels, and images of the gels spotted onto the TEM grids were then captured by TEM. The TEM images demonstrate the extensive formation of nanofibers, presumably resulting from intercolumnar associations of the 1D H-aggregates, for **2** in *n*-hexane (Figure 3a), ethyl acetate (Figure 3b), and cyclohexane (Figure 3c). These seemingly endless nanofibers typically measure between 100 and 250 nm in width and are structured in a 3D knotted network able to "freeze" solvent molecules to form the gel. For **3**, fiber formation is also observed in ethyl acetate (Figure 3d) and *n*-hexane (Figure S26) even though the image quality seems not to be very excellent.

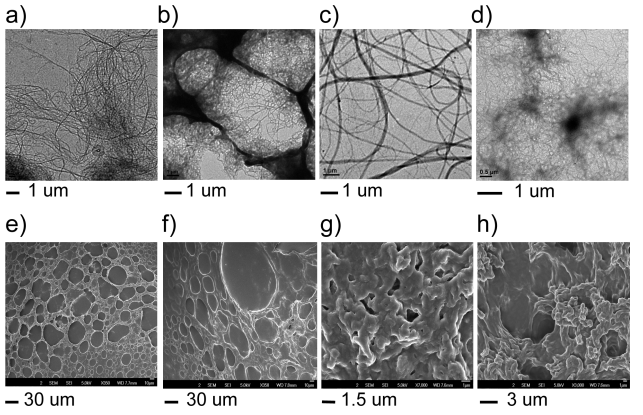

Figure 3. TEM images of the as-formed gels of **2** in (a) *n*-hexane, (b) ethyl acetate, and (c) cyclohexane and (d) of **3** in ethyl acetate as well as SEM micrographs of the as-formed gels of (e) **2** in *n*-hexane, (f) **3** in *n*-hexane, (g) **2** in ethyl acetate, and (h) **3** in ethyl acetate.

A micromorphological investigation by scanning electron microscopy (SEM) reveals similar surface topographies in the microstructure of the gels formed from the same solvent (Figure 3e–3h). While a highly porous surface with a three-dimensional lattice of many voids and possibly channels is found for gels formed by both **2** and **3** in *n*-hexane (Figure 3e and 3f), a smoother surface with significantly less voids embedded within the 3D lattice appears for those formed in ethyl acetate by **2** or **3** (Figure 3g and 3h). Such an increase in porosity for gels formed in *n*-hexane possibly may enhance the retention of solvent molecules, accounting for the lower MGC values in *n*-hexane compared to those in ethyl acetate (Table 1).

To establish the 3D arrangement of 1D H-aggregates responsible for the fiber formation, powder X-ray diffraction (XRD) analysis was carried out. However, the obtained XRD data are of low resolution and do not allow for the unambiguous assignment of the packing pattern by 1D columns.[8] Still, the presence of predominant major peaks below 5° (Figures S27 and S28) may allow us to estimate the interpenetrating depth by exterior side chains. From $2\theta = 3.70°$ in Figure S28 for pentamer **3**, the value of d_{100} spacing for gels formed by pentamer **3** can be calculated to be 23.86 Å, corresponding to an intercolumnar distance of $d_{hex} = 2.76$ nm or $d_{tetra} = 3.37$ nm, respectively, for the hexagonal and tetragonal arrangements that are the two most common packing patterns. In light of a radius of ~2.13 nm for the 1D columns formed from **3** (0.68 nm from its pentamer core plus 1.45 nm from its dodecyl side chain), the overlapping among the 1D columns can be calculated to be about 0.75 and 0.45 nm, respectively, for the hexagonal and tetragonal arrangements. This suggests that the exterior dodecyl side chains may possibly penetrate into each other by a four- to seven-carbon linker length.

Similarly, on the basis of the value for $d_{100} = 18.70$ Å ($2\theta = 4.72°$, Figure S27) for gels formed by **2** and an overall radius of 1.65 nm for the 1D columns by **2**, an intercolumnar distance of $d_{hex} = 2.16$ nm and $d_{tetra} = 2.64$ nm and so an overlapping of 0.57 and 0.33 nm among the exterior octyl side chains, respectively, for the hexagonal and tetragonal arrangements can be estimated, suggesting that it is highly likely that the octyl side chains penetrate into each other by a three- to five-carbon linker length.

In summary, a crystallographic observation of the H-bond enhanced intermolecular aggregation occurring in a 2D-shaped macrocyclic fluoropentamer enables us to design two macrocyclic organogelators with high gelling abilities in organic solvents such as hexane, cyclohexane, ethyl acetate, and dioxane. Experimental analyses based on TEM and XRD data suggest that the gelling networks contain 3D entangled nanofibers formed from the intercolumnar association of 1D H-aggregates possibly via hydrophobic interactions among interpenetrating alkyl side chains. These fluoropentamers represent rare examples of 2D-shaped macrocyclic organogelators.

Acknowledgment. Financial support of this work to H.Z. by the NUS AcRF Tier 1 grants (R-143-000-375-112 and R-143-000-398-112) and A*STAR BMRC research consortia (R-143-000-388-305) is gratefully acknowledged.

Supporting Information Available. Synthetic procedures and a full set of characterization data including ^{1}H NMR, ^{13}C NMR, HRMS, and crystal data. This material is available free of charge via the Internet at http://pubs.acs.org.

(8) The XRD data of the gels formed from **2** and **3** differ significantly from the XRD of single crystals of **1** (Figure S29) that packs hexagonally in a 2D space but not in a 3D space. Comparison of XRD data among **1**–**3** does not permit us to confidently deduce the possible arrangements of 1D columns formed by **2** and **3**.